PHYSICAL REVIEW B VOLUME 49, NUMBER 10 1 MARCH 1994-II

Free-volume microstructure of amorphous polycarbonate at low temperatures determined by positron-annihilation-lifetime spectroscopy

J. Krištiak
Institute of Physics, Slovak Academy of Sciences, Dúbravská cesta 9, 84228 Bratislava, Slovakia

J. Bartoš
Polymer Institute, Slovak Academy of Sciences, Dúbravská cesta 9, 84236 Bratislava, Slovakia

K. Krištiaková, O. Šauša, and P. Bandžuch
Institute of Physics, Slovak Academy of Sciences, Dúbravská cesta 9, 84228 Bratislava, Slovakia

(Received 24 September 1993)

Amorphous polycarbonate has been investigated from the point of view of free-volume microstructure in the temperature range 50–350 K by positron-annihilation-lifetime spectroscopy. Lifetime τ_3 and relative intensity I_3 of *o*-Ps show two regions of different behavior with the transition at $T_b = 130$ K. The temperature dependence of τ_3 has been analyzed using the model of a particle in a spherical potential well. The correlations between the dilatometric measurements and the $\tau_3(T)$ and $I_3(T)$ dependences have been interpreted in the framework of the free-volume model, which allowed us to estimate the fraction of free volume accessible to *o*-Ps as well as the concentration of free-volume entities. We have determined that the polycarbonate is a relatively defect-full material. On the basis of a simple thermodynamical approach allowing for simultaneous change of the size and number of free-volume entities, an attempt has been made to specify the molecular mechanism responsible for the free-volume changes. The comparison of the results of such a thermodynamical model with the simulation of the structure of amorphous polycarbonate and the dynamics of the motion of phenyl groups suggests that partial flips of this group might be the potential generators of the increased free volume at $T > T_b$.

I. INTRODUCTION

The concept of the free-volume structure of solids and subsequently the correlation between free volume and the physical properties of solids and its interpretation is a very useful and popular idea in the physics of disordered systems[1] and especially of polymers.[2–4] It is generally accepted that free volume determines the polymer dynamics, which is one of the crucial aspects in mechanical and transport phenomena. Thus it is very important to quantify free volume, not only by its integral value but also to determine the distribution of free-volume entities.

Conventional experimental techniques such as small-angle x-ray scattering,[5,6] photochromic, fluorescence,[7,8] and electron spin resonance (ESR)[9] spectroscopies may provide estimates of the sizes of holes; however, this is usually possible only on a relatively large scale above 1 nm, or only indirectly due to the relatively large sizes of the labeling and probing entities, or the information about the second momentum of free-volume distributions is provided through density fluctuations.[10,11] The only technique capable at present of measuring directly free-volume entities on the atomic scale is positron-annihilation spectroscopy.[12] This method is based on the fact that the positron lifetime is very sensitive to the presence of defects and inhomogeneities in the matrix.[13,14] In the case of nonconductive molecular materials such as polymers, besides the annihilation of the positron, there takes place also the formation and annihilation of positronium Ps, i.e, the bound state of e^+ and e^- with atomic radius comparable to that of the hydrogen atom. Ps exists in two states depending on the mutual spin orientation of e^+ and e^-. Para-Ps (*p*-Ps) annihilates with lifetime $\tau_1 = 0.125$ ns in vacuum; the triplet ortho-Ps (*o*-Ps) with parallel spins has a lifetime τ_3 in vacuum of 142 ns. In a condensed medium, the value of τ_3 is lowered to a few nanoseconds, due to interaction with surrounding electrons by the so-called pick-off process, which is strongly dependent on the electron density of the immediate microsurroundings around the *o*-Ps. It seems that *o*-Ps prefers surroundings with lower electron density, i.e., free volumes. A simple quantum-mechanical model of positronium in a spherical potential well provides the relation between the value τ_3 and the radius of the hole R as[15]

$$\tau_3 = \tfrac{1}{2}[1 - R/R_0 + (1/2)\pi \sin(2\pi R/R_0)]^{-1} , \qquad (1)$$

where R is the radius of a spherical hole, $R_0 = R + \Delta R$. The thickness of the electron layer $\Delta R = 1.656$ Å is obtained from fitting the experimental values of τ_3 obtained from materials with known hole size, e.g., zeolites.

Polycarbonate is an important material for engineering, interesting because of its mechanical properties such as impact strength and their dependence on the thermomechanical history of the material. This is why it has been one of the polymers selected for investigation by the positron-annihilation-spectroscopy (PAL) method.[16–19] Previous studies presented changes in the lifetime τ_3 and the intensity I_3 in the higher temperature range around

0163-1829/94/49(10)/6601(7)/$06.00

$T_g = 150\,°\mathrm{C}$ and $T_\beta = 50\,°\mathrm{C}$ with the emphasis on thermal annealing below and above T_g.[16–18] The work of Kluin *et al.*[18] indicates the presence of a distribution of hole sizes in a polycarbonate. In this work a comparison of the thermal expansivity of the vacancies and of their macroscopic value was also performed, giving a free-volume fraction of 8% at a temperature of 150 °C. The mechanical influence on the free-volume microstructure has been investigated at room temperature in the linear region of the deformation regime.[19] According to our best knowledge, no low-temperature studies of the polycarbonate have been performed in the very interesting γ-relaxation region, which would be of fundamental importance for microstructural characterization and subsequent understanding of the entire complex of physicochemical properties, such as relaxation, regimes of tensile behavior, etc.

II. EXPERIMENTAL

A Bis-phenol-A-based amorphous polycarbonate (BPA-PC), the product name Makrolon [Bayer (Germany)] with $M_W = 3.2 \times 10^4$ has been used as sample. The glass transition temperature $T_g = 150\,°\mathrm{C}$ has been determined using differential scanning calorimetry with heating rate 20 °C/min.

Samples for PAL measurements were in the form of disks with 10 mm diameter, ~5 mm thick. The positron source ^{22}NaCl was deposited in an envelope of Kapton foils (8 μm thick). It was then sandwiched in between two identical pieces of the samples. This assembly was completely enclosed in a copper sample holder at the end of the cold finger of a closed-cycle helium gas refrigerator with automatic temperature regulation. Each selected temperature was kept constant within ±0.5 °C during data acquisition. The entire source-sample assembly was kept in vacuum. The measurements were carried out in the following sequences:

(i) immediately after source installation at 293 K;

(ii) next the temperature was lowered to ~50 K and then was raised to 350 K in steps of 10 K. Lifetime spectra were obtained within 60 min at each temperature. At least two sets of such measurements have been performed.

We employed a standard lifetime spectrometer with plastic scintillators coupled to Philips XP2020 photomultipliers. Ortec 583 constant fraction discriminators were used for selecting the energy and providing timing signals to a time-to-amplitude converter. The time resolution [full width at half maximum (FWHM)] of prompt spectra was 320 ps. A model-independent estimate of the instrument resolution function was obtained from the decay curve of the ^{207}Bi isotope with a single lifetime of 182 ps. These ^{207}Bi data have been used in conventional data analysis (fit of several exponentials). The time spectra have ~5×10^5 total counts.

In conventional analysis the PATFIF-88 program of Kirkegaard *et al.*[20] was employed. A source correction term was subtracted from each spectrum. This correction has been deduced from the analysis of time spectra ($\tau = 382$ ps, $I = 4.8\%$) taken on an annealed Al sample. The resolution function was approximated as a sum of three Gaussians. Three- as well as four-component analyses of data were performed. The four-component description of data gives an error for the intensity of the third component (~900 ps) comparable to the intensity itself.

III. RESULTS AND DISCUSSION

Experimental results from positron-annihilation-lifetime spectroscopy in amorphous polycarbonate as a function of temperature in the temperature interval from 50 to 350 K are shown in Figs. 1 and 2. The lifetime τ_3 and relative intensity I_3 of the *o*-Ps exhibit analogous temperature dependences, consisting of two linear regions with very differing behavior. In the temperature region below $T_b = 130$ K, both characteristics are practically constant; above T_b, however, they increase linearly with increasing temperature. Empirical relations describing these results are the following:

$$\tau_3(T) = (2.071 \pm 0.108) \times 10^{-3}(T - T_b) + (1.758 \pm 0.031)[\mathrm{ns}]\,, \tag{2}$$

$$I_3(T) = (33.1 \pm 6.5) \times 10^{-3}(T - T_b) + (17.2 \pm 1.9)[\%]\,. \tag{3}$$

The average hole sizes $\bar{V}_{\mathrm{hole}}$ determined according to the semiempirical model, Eq. (1), are plotted on the right-hand scale in Fig. 1. Note that the hole size attains approximately one-third to one-half of the van der Waals volume of the basic structural unit of the polycarbonate (230.2 Å^3).

The slopes of the linear dependences of lifetimes and hole volumes on temperature are used to calculate the temperature coefficients, defined as

$$\alpha_\tau(T) = \frac{1}{\tau_3(T)} \frac{\Delta\tau_3}{\Delta T} \quad \text{or} \quad \alpha_h(T) = \frac{1}{\bar{V}_h(T)} \frac{\Delta\bar{V}_h}{\Delta T}\,.$$

While in the low-temperature region (region I) both coefficients are zero, their values for intermediate temperature in the interval from 130 to 300 K (region II), i.e., 215 K, are $\alpha_\tau^{\mathrm{II}} = 1.07 \times 10^{-3}\ \mathrm{K}^{-1}$ or $\alpha_h^{\mathrm{II}} = 2.13 \times 10^{-3}\ \mathrm{K}^{-1}$.

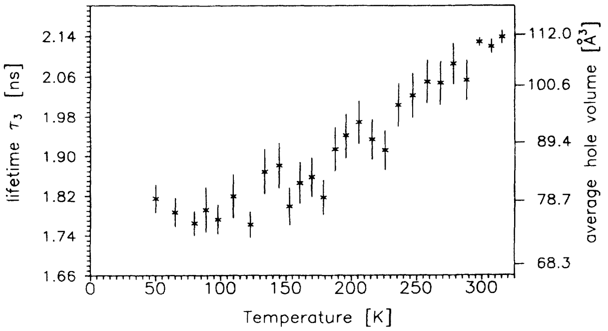

FIG. 1. Lifetime of *o*-Ps, τ_3, as a function of temperature in amorphous polycarbonate. The hole size $\bar{V}_{\mathrm{hole}}$ is plotted on the right-hand side.

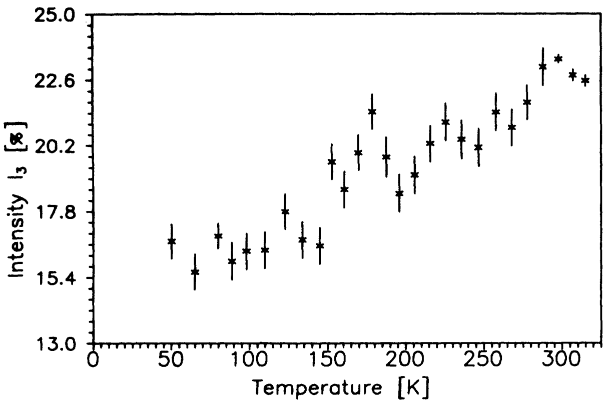

FIG. 2. Relative intensity of *o*-Ps, I_3, as a function of temperature in amorphous polycarbonate.

From dilatometric measurements on polycarbonate in the temperature region investigated[21,22] follow also the existence of two temperature intervals with temperature coefficients of expansion defined as

$$\alpha_V(T)=\frac{1}{V(T)}\frac{\Delta V}{\Delta T}\ ,$$

with values of $\bar{\alpha}_V^{\mathrm{I}}=1.11\times10^{-4}\ \mathrm{K}^{-1}$ and $\bar{\alpha}_V^{\mathrm{II}}=1.81\times10^{-4}\ \mathrm{K}^{-1}$.[22] The onset of transition between the two regions can be determined more exactly from the $\alpha_V(T)$ dependences; it is situated at 132 K (Fig. 11, Ref. 21) or at 138 K (Fig. 12, Ref. 22). From the correlation between the onset of the change of temperature coefficient of expansion of macroscopic volume and the temperature of the break, $T_b=130$ K determined by PAL, it can be assumed that the onset of faster change of macroscopic volume is in direct relation with the changes in microscopic free-volume relations.

The qualitative picture following from dilatometric and positron-annihilation measurements is as follows. For $T<T_b$ the macroscopic volume increases slowly with increasing temperature; the free-volume microstructure is, however, preserved. This means that below 130 K there exists a static hole structure of the polymer, that is, the frozen-in defect structure of the matrix with a certain quasistatic free-volume fraction $f^a(T)>0$. From this it follows that thermal expansion can take place only via anharmonic motions of chains, which means that only the oscillation expansion mechanism is active. Above T_b a more pronounced change of macroscopic volume takes place due to the change of the average size and population of holes, as detected by the PAL method. In this case the volume expansion is realized via anharmonic motions as well as via the growth of the average size and concentration of holes, which represents the so-called oscillation-and-defect mechanism of the volume expansion of the polycarbonate.

The quantitative description of the dilatometric and positron-annihilation data is based on the separation of macroscopic volume $V(T)$ into two parts:

$$V(T)=V_f^a(T)+V_{\mathrm{rest}}(T)\ , \tag{4}$$

where $V_f^a(T)$ is the part of the total free volume of the matrix accessible to *o*-Ps and $V_{\mathrm{rest}}(T)$ is the remaining volume, consisting of the van der Waals volume of the particles V_W, which is practically temperature independent, the vibrational contribution $V_{\mathrm{vibr}}(T)$, and the part of the total free volume V_f^b inaccessible to *o*-Ps due to geometrical and/or dynamic reasons. Using the definition of the fractional hole volume

$$f_h^a(T)=\frac{V_f^a(T)}{V(T)}\ , \tag{5}$$

we obtain the relation between the macroscopic volume change and the change of the microscopic free volume

$$\alpha_V(T)=f_h^a(T)\alpha_h(T)+[1-f_h^a(T)]\alpha_{\mathrm{rest}}(T)\ , \tag{6}$$

from which we can determine the fraction of the free volume detectable by the PAL method,

$$f_h^a(T)=\frac{\alpha_V(T)-\alpha_{\mathrm{rest}}(T)}{\alpha_h(T)-\alpha_{\mathrm{rest}}(T)}\ . \tag{7}$$

Due to static free-volume behavior it is convenient in the low-temperature region to put $\alpha_{\mathrm{rest}}=\alpha_V^{\mathrm{I}}$, and thus $f_h^a=0$. This means that in this definition f_h^a has the significance of the dynamic contribution f_h^{ad} to the already existing quasistatic free-volume fraction f_h^a for $T\le T_b$. This separation and comparison of the macroscopic volume and free-volume relations is depicted in Fig. 3. The additional free-volume contribution related to the dynamic character of the free-volume microstructure is nonzero only in the region $T>T_b$. The magnitude of f_h^{ad} can be determined from Eq. (7) using the published dilatometric[22] and the present positron-annihilation data. The magnitude of f_h^{ad} has been determined for the mean

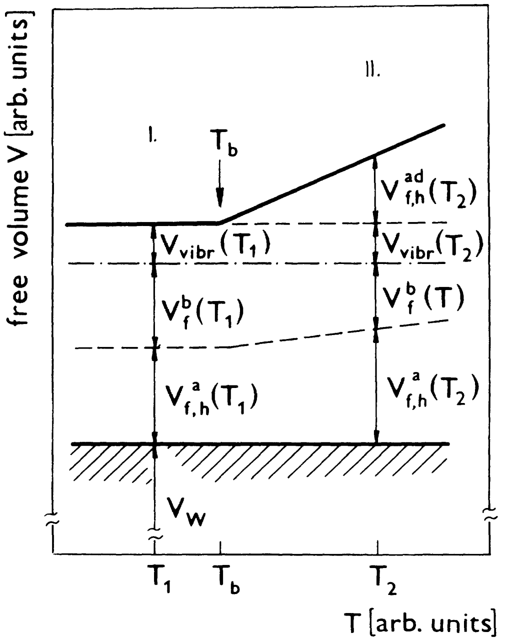

FIG. 3. Schematic illustration of the decomposition of macroscopic volume of a polymer. V_W: van der Waals volume; V_{vibr}: volume due to vibrations; V_f^b: free volume inaccessible to *o*-Ps; V_f^a: free volume accessible to *o*-Ps.

temperature $\bar{T}=215$ K corresponding to the interval from 130 K to 300 K, and it is equal to 0.035.

If the relative intensity I_3 is proportional to the number of holes, then it holds that the fractional free volume is given by the product[23]

$$f_h(T)=C(T)\tau_3(T)I_3(T) .$$

This relation can then be used to estimate the fraction of the quasistatic free volume $f_h^a(T)$ and then to estimate the total fraction of the free volume $f_h(T)$. Using the assumptions that the coefficient C does not depend on the temperature and that the quasistatic free volume V_f^a for $T>T_b$ accessible to *o*-Ps changes proportionally with the change of the total macroscopic volume, we can write

$$f_h^a(T_1)=f_h^{ad}(T_2)\frac{\tau_3(T_1)I_3(T_1)}{\tau_3(T_2)I_3(T_2)-\tau_3(T_1)I_3(T_1)} , \tag{8}$$

and from known values of τ_3 and I_3 we can estimate the f_h^a part of the whole fraction f_h accessible to *o*-Ps. Using linear representations for τ_3 and I_3 according to Eqs. (2) and (3), for temperatures $T>T_b$ we obtain the result that the fraction of the quasistatic free volume in the polycarbonate at $T_b=130$ K amounts to 12.6%.

The alternative way of calculation makes use of a combination of empirical and semiempirical parameters[24,25] in the relation $f_h(T)=D(T)\bar{V}_h(T)I_3(T)$. Under the same assumptions as above and using a relation analogous to Eq. (8) we obtain a slightly lower value $f_h^a(130\text{ K}) = 9.2\%$. In our further considerations we shall be using the former approach because of its purely empirical origin.

It is interesting to compare the estimate of the quasistatic free-volume fraction from the PAL measurements with the total free volume determined by the Bondi method.[26] According to this method, the fractional empty free volume at any temperature is defined as

$$f^e(T)=\frac{V(T)-V_W}{V(T)} , \tag{9}$$

and for $T=0$ K it has the meaning of the structural (true static) free volume. Using dilatometric data from Ref. 22, and the Askadskij approach[27] to the calculation of V_W, we can find that $f^e(130\text{ K}) = 0.322$. Note that $f^e(T>0\text{ K})$ represents the maximum free volume in a system without any motion. Thus, *o*-Ps is capable of identifying at least about 39% of the empty volume at 130 K. From this it follows that the rest corresponds to the free-volume entities which are smaller than the size of the *o*-Ps, as well as to the portion of the entities sufficiently large to trap *o*-Ps but having a frequency of motion of the order of $\nu>10^9$ s. The fractions of the total free volume recorded by the PAL method and estimated according to the above-outlined procedure are listed for the three temperatures investigated in Table I.

The magnitude of the dynamic contribution $f_h^{ad}(25\,^\circ\text{C})=6.7\%$ agrees with the value of 8% deduced from the data of Kluin *et al.*[18] for $T=150\,^\circ\text{C}$.

The complete characterization of the free-volume microstructure detectable by the PAL technique requires the knowledge of two parameters, namely the mean size of the free-volume entities $\bar{V}_h(T)$ and their mean concentration $\bar{c}_h(T)$. While the first quantity is obtainable by applying Eq. (1), the second one can be calculated from the estimated free-volume fractions. Table I lists some of the possibilities of expressing the hole concentrations, all of them based on the definition.

$$f_h(T)=\bar{c}_h^V(T)\bar{V}_h(T) , \tag{10}$$

where $\bar{c}_h^V(T)$ is the volume concentration of the holes, with the mean volume $\bar{V}_h(T)$ determined from the lifetime $\tau_3(T)$. The mass or molar concentration of the holes is obtained from the specific volume $V(T)$ and molar mass M of the polycarbonate, $M=254$ g/mole. From Table I it is evident that with increasing temperature the total hole concentration for $T>T_b$ increases. Physically the most illustrative case seems to be the determination of the number of holes per monomer unit. This quantity shows that on average there is approximately 1 hole per 2 monomer units in the whole temperature range investigated. An alternative representation of the concentration relations of holes resides in the estimate of the mean volume corresponding to a single hole $\bar{v}$ as well as the mean distance $\bar{l}_h$ between the holes, assuming their homogeneous distribution in the polymer. The last two columns in Table I make it evident that, while the mean volume in which one hole is localized decreases with temperature, the mean distance between neighboring holes changes relatively little. As for the dynamically generated free volume for $T>T_b$, the temperature dependence of

TABLE I. Characteristics of the hole concentration c at three temperatures in amorphous polycarbonate.

T (K)	$V^{\text{dil a}}$ (cm^3/g)	$V_{\text{hole}}^{\text{PAL}}$ (cm^3/hole)	f_h	$\bar{c}_h^m$ (hole/g)	$\bar{c}_h^{\text{mole}}$ (hole/mole)	$\bar{c}_h^{\text{mon}}$ (hole/mon)	$\bar{c}_h^v$ (hole/cm^3)	$\bar{v}=\frac{1}{\bar{c}_h^v}$ (Å^3/hole)	$\bar{l}_h$ (Å/hole)
130 (T_b)	0.805	7.6×10^{-23}	0.126	1.34×10^{21}	3.39×10^{23}	0.560	1.66×10^{21}	608	8.5
215	0.817	9.1×10^{-23}	0.161	1.45×10^{21}	3.67×10^{23}	0.610	1.77×10^{21}	566	8.3
			=0.126	1.13×10^{21}	2.87×10^{23}	0.480	1.39×10^{21}	720	9.0
			+0.035	3.14×10^{20}	8.00×10^{22}	0.130	3.85×10^{20}	2600	13.8
300 (RT)	0.833	10.9×10^{-23}	0.193	1.48×10^{21}	3.35×10^{23}	0.620	1.77×10^{21}	565	8.3
			=0.126	9.63×10^{20}	2.45×10^{23}	0.410	1.16×10^{21}	865	9.5
			+0.067	5.12×10^{20}	1.30×10^{23}	0.220	6.15×10^{20}	1627	11.8

[a] From Ref. 22, dil is dilatometric, mon is monomer.

the mean distance between holes is stronger and decreases from 14 to 12 Å. These conclusions are related to the fact that a substantial portion of the free volume is formed by the "quasistatic" contribution, which represents 3/4 and 2/3 of the total accessible free volume at 215 K and at 300 K, respectively.

From the above comparison of the results from dilatometric and positron-annihilation measurements for $T > T_b$, it follows that the free-volume microstructure in this region has dynamic character, mean size as well as mean concentration of the holes changing simultaneously with changing temperature.

Next, we try to analyze this temperature region from the thermodynamic point of view with the aim of revealing the molecular causes of these changes. We present a model which is based on the following assumptions:

(i) the existence of dynamical equilibrium between formation and decay of holes,

(ii) the activated character of the process of formation and decay of holes, i.e., the activation concept of the processes, and

(iii) the existence of a homogeneous structure of holes, i.e., zero size distribution.

According to the scheme of dynamical equilibrium between formation and decay of holes,

$$\text{no hole} \underset{k_d}{\overset{k_f}{\rightleftharpoons}} \text{hole}\ , \tag{11}$$

the equilibrium constant is given by

$$K(T) = \frac{k_f(T)}{k_d(T)}\ , \tag{12}$$

where $k_f(T)$ and $k_d(T)$ are rate constants for the formation and decay processes, respectively. In accordance with assumption (ii), both rate constants can be expressed in the Arrhenius form $k_f(T) = k_{0f}\exp(-E_f^*/RT)$ and $k_d(T) = k_{0d}\exp(-E_d^*/RT)$. Furthermore, with regard to the relation between the mean activation energies $\bar{E}_f^* = \bar{E}_d^* + \Delta\bar{H}$, where $\Delta\bar{H}(T)$ is the mean energy of hole formation, we can write

$$K(T) = \exp\left[-\frac{\Delta\bar{H}}{RT}\right]\ . \tag{13}$$

Then in the case of simultaneous change of mean size and number of holes, we obtain for the ratio of equilibrium rate constants at two temperatures

$$\frac{K(T_2)}{K(T_1)} = 1/\exp\left[\frac{\Delta\bar{H}_{h2}}{R}\left[\frac{1}{T_2} - \frac{1}{T_1}\right]\right]\exp\frac{\Delta\bar{H}_{h21}}{RT_1}\ , \tag{14}$$

where $\Delta\bar{H}_{h21}$ is the change (decrease) of the mean hole size upon the change (decrease) of the temperature from T_2 to T_1.

Equilibrium hole constants can be expressed also as

$$\frac{K(T_2)}{K(T_1)} = \frac{N_h(T_2)}{N_h(T_1)}\ , \tag{15}$$

where $N_h(T)$ is the number of holes at temperature T.

Using the frequently accepted assumption[28] that $I_3 \sim N_h$, the PAL parameter can be related to the energetic hole characteristics,

$$\frac{I_3(T_2)}{I_3(T_1)} = 1/\exp\left[\frac{\Delta\bar{H}_{h2}}{R}\left[\frac{1}{T_2} - \frac{1}{T_1}\right]\right]\exp\frac{\Delta\bar{H}_{h21}}{RT_1}\ . \tag{16}$$

The results obtained from molecular-mechanical simulation of the amorphous polycarbonate[29] can be used in the search for the meaning of the quantities of the model presented. Investigations of the dynamics of the phenyl chains in the bulk state have shown[30] that full rotation at room temperature takes place as a two-barrier process, while the typical energy difference between two local minima amounts to 16.8 kJ/mole (Fig. 5 from Ref. 30). Then, assuming that a partial flip motion of the phenyl ring is the potential mechanism for the formation of the free volume, the mean energy difference between the two local minima can be estimated at the onset of the dynamical region at $T_b = 130$ K using the experimental intensities measured at 293 and 130 K and Eq. (16). The estimate amounts to some 8 kJ/mole, i.e., a decrease of conformation energy should take place with decrease of temperature. This result seems to be a paradox in view of the mean-field approximation; however, it is well understandable from the viewpoint of the concept of inhomogeneous glassy structure of the polycarbonate matrix. Figure 4 displays the rotation-energy diagram for the full rotation

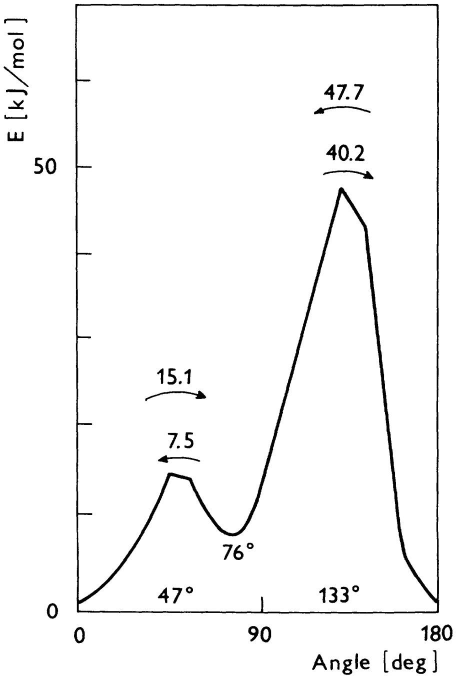

FIG. 4. Rotational-energy diagram of phenyl group rotation in an isolated fragment of polycarbonate.

of the phenyl group in an isolated polycarbonate chain, obtained using computer software.

Molecular modeling of the motion of the phenyl chain in isolated polycarbonate fragments has been realized using the program INSIGHT for construction of the molecule and the program MOPAC (QCPE) for calculation of the rotation-energy diagram. The computations have been performed on a Silicon Graphics IRIS 4D/70GT work station.

From comparison with the analogous diagram for the identical process in the bulk state at room temperature[31] it follows that the double-barrier character of the process is preserved, while the energy difference between the two local minima is lowered to 7.5 kJ/mole. The value estimated from the thermodynamic model at $T_b = 130$ K is close to the value for the isolated state, which could indicate that a partial flip of the phenyl ring by $\sim 75°$ might be the effective degree of freedom responsible for the generation of the free volume. Then, according to this picture, the free-volume entities could form at first in the less dense regions of the matrix at low temperatures, and then with increasing temperatures formation could occur in increasingly more dense zones of the polymer. The plausibility of the phenyl motion being the generator of the free volume could be supported by results from special NMR experiments with deuterated phenyl rings. These NMR results on polycarbonate suggest the existence of low-angle high-frequency motions of the rings as well as of large-amplitude flip motions in the low-temperature region.[31–33] Similarly, simulation computations[30] point to a broad distribution of activation energies and frequencies of the flip motions, which reflect a significant variability of the neighborhoods of the aromatic rings.

Our observations seem to be consistent with these results and contribute to the overall picture of the structural and dynamical relations in amorphous polycarbonate in the low-temperature region. We suppose that knowledge of microstructural free-volume relations in the form of the mean size of holes and mean concentration of holes, as provided by the PAL method, is a necessary prerequisite for understanding of the microscopic basis of various phenomena, above all, relaxation, mechanical and transport phenomena. The next step in the characterization of microstructural relations is polycarbonate is the determination of the free-volume distribution and its change with temperature[34] and with other parameters. Work in this direction is in progress.

IV. CONCLUSIONS

This work presents the results of measurements of positronium lifetime τ_3 and its relative intensity I_3 in amorphous polycarbonate in the temperature interval from 50 to 350 K. A free-volume model has been proposed which allows us to estimate from the temperature dependences $\tau_3(T)$ and $I_3(T)$ the free-volume fractions accessible to *o*-Ps as well as the corresponding concentration of these free-volume entities. A thermodynamical model has been formulated which, in combination with the data from simulations presented in the literature, allows us to discuss potential molecular reasons for the free-volume changes in the dynamical region above 130 K.

ACKNOWLEDGMENT

This work was supported, in part, by the Grant Agency for Science.

---

[1] R. Zahlen, *The Physics of Amorphous Solids* (Wiley, New York, 1986).
[2] J. D. Ferry, *Viscoelastic Properties of Polymers*, 3rd ed. (Wiley, New York, 1980).
[3] R. N. Haward, *The Physics of Glassy Polymers* (Wiley, New York, 1973).
[4] G. B. McKenna, in *Polymer Properties*, edited by C. Booth and C. Price, *Comprehensive Polymer Science*, Vol. 2 (Pergamon, Oxford, 1990).
[5] W. Wiegand and W. Ruland, Prog. Colloid Polym. Sci. **66**, 355, (1978).
[6] Y. Tanaka, N. Müller, and E. W. Fischer, Polym. J. **16**, 1445 (1984).
[7] J. G. Victor and J. M. Torkelson, Macromolecules **20**, 2241 (1992).
[8] W. Ch. Yu, Ch. S. P. Sung, and R. E. Robertson, Macromolecules **21**, 355 (1988).
[9] F. D. Tsay and A. Gupta, J. Polym. Sci. B **25**, 855 (1987).
[10] J. H. Wendorff, E. W. Fischer, and Z. Z. Koll, Polymer **251**, 876 (1973); **251**, 884 (1973).
[11] H. H. Song and R. J. Roe, Macromolecules **20**, 2723 (1987).
[12] Y. C. Jean, Microchem. J. **42**, 72 (1990).
[13] *Positron Solid-State Physics*, edited by W. Brandt and A. Dupasquier (North-Holland, Amsterdam, 1983).
[14] *Positron and Positronium Chemistry*, edited by D. M. Schrader and Y. C. Jean (Elsevier, Amsterdam, 1988).
[15] H. Nakanishi and Y. C. Jean, in *Positron and Positronium Chemistry* (Ref. 14), p. 95–103.
[16] A. J. Hill, P. L. Jones, J. H. Lind, and G. W. Pearsall, J. Polym. Sci. A **26**, 1541 (1988).
[17] A. J. Hill, I. M. Katz, and P. L. Jones, Polym. Eng. Sci. **30**, 762 (1990).
[18] J. E. Kluin, Z. Yu, S. Vleeshouwers, J. D. McGervey, A. M. Jamieson, and R. Simha, Macromolecules **25**, 5089 (1992).
[19] M. Y. Ruan, H. Moadell, A. M. Jamieson, R. Simha, and J. D. McGervey, Macromolecules **25**, 2407 (1992).
[20] P. Kirkegaard, N. Y. Pedersen, and M. Eldrup (unpublished).
[21] J. M. Roe and R. Simha, Int. J. Polym. Mater. **3**, 193 (1974).
[22] R. Greiner and F. R. Schwarzl, Rheol. Acta **23**, 378 (1984).
[23] Y. Y. Wang, H. Nakanishi, Y. C. Jean, and T. C. Sandreczki, J. Polym. Sci. B **28**, 1431 (1990).
[24] Y. Kobayashi, W. Zheng, E. F. Meyer, J. D. McGervey, A. M. Jamieson, and R. Simha, Macromolecules **22**, 2302 (1989).
[25] H. Nakanishi, Y. C. Jean, E. G. Smith, and T. C. Sandreczki, J. Polym. Sci. B **27**, 1419 (1989).
[26] A. Bondi, J. Phys. Chem. **58**, 929 (1954).
[27] A. A. Askadskij, Usp. Khim. **46**, 1122 (1977).
[28] K. Venkateswaran, K. L. Cheng, and Y. C. Jean, J. Phys.

Chem. **88**, 2465 (1984).

[29] M. Hutnik, F. T. Gentile, P. J. Ludovice, U. W. Suter, and A. S. Argon, Macromolecules **24**, 5962 (1991).

[30] M. Hutnik, A. S. Argon, and U. W. Suter, Macromolecules **24**, 5970 (1991).

[31] H. W. Spiess, Colloid Polym. Sci. **261**, 193 (1983).

[32] M. Wehrle, G. P. Hellmann, and H. W. Spiess, Colloid Polym. Sci. **265**, 815 (1987).

[33] H. W. Spiess, Adv. Polym. Sci. **66**, 24 (1985).

[34] J. Krištiak, K. Krištiaková, O. Šauša, P. Bandžuch, and J. Bartoš, J. Phys. (Paris) **3**, 265 (1993).